Magnetic field strength in solar coronal waveguides

I. Arregui[1,2] **and A. Asensio Ramos**[1,2]

[1] Instituto de Astrofísica de Canarias, Vía Láctea s/n, E-38205 La Laguna, Spain
[2] Departamento de Astrofísica, Universidad de La Laguna, E-38206 La Laguna, Spain

Abstract

We applied Bayesian techniques to the problem of inferring the magnetic field strength in transversely oscillating solar coronal loops from observed periods and damping times. This was done by computing the marginal posterior probability density for parameters such as the waveguide density, the density contrast, the transverse inhomogeneity length scale, and the magnetic field strength under the assumption that the observed waves can be modelled as standing or propagating magnetohydrodynamic (MHD) kink modes of magnetic flux tubes. Our results indicate that the magnetic field strength can be inferred, even if the densities inside and outside the structure are largely unknown. When information on plasma density is available, the method enables to self-consistently include this knowledge to further constrain the inferred magnetic field strength. The inclusion of the observed oscillation damping enables to obtain information on the transverse density structuring and considerably alters the obtained posterior for the magnetic field strength.

1 Coronal seismology: from classic to Bayesian techniques

Coronal seismology uses observed and theoretically predicted properties of magnetohydrodynamic (MHD) waves and oscillations to infer plasma and field properties. The method was suggested long ago by [8], [7], and [6]. Coronal seismology using transverse oscillations was first applied by [4] using observations made by the Transition Region and Coronal Explorer (TRACE) and reported by [2] and [5] to infer the magnetic field strength in oscillating coronal loops. The observed lateral displacements of coronal loops were interpreted as being due to the presence of the fundamental MHD kink mode of a magnetic flux tube. By estimating the phase speed of the waves and associating this observable to the theoretical kink speed, the magnetic field strength could be determined, upon making a number of assumptions on the values of the plasma density inside and outside the coronal loops. Coronal loop oscillations display time damping and [1] were the first to self-consistently include this information in the determination of physical parameters of coronal loops.

In contrast to the situation in a laboratory, the study of the solar atmosphere has to be pursued without direct access to the physical conditions of interest. Information is therefore incomplete and uncertain and the inference of physical parameters is a typical problem in which a probabilistic approach has to be followed. Probabilistic inference considers any inversion problem as the task of estimating the degree of belief on statements about parameter values, conditional on observed data. It uses Bayes theorem which says that our state of knowledge on a given parameter set, θ, conditional on the observed data, D, and the assumed theoretical model, M, is a combination of what we know independently of the data, the prior $p(\theta|M)$, and the likelihood of obtaining the observed data as a function of the parameter vector, $p(D|\theta, M)$. Their combination leads to the posterior, $p(\theta|D, M)$, which encodes all the available information about the unknown parameters. Once the full posterior is known, information on a particular parameter can be obtained by performing an integral of the posterior with respect to the remaining parameters to obtain the so-called marginal posterior.

This paper shows results from the application of Bayesian probability to the problem of inferring the magnetic field strength in transversely oscillating coronal waveguides, under different knowledge circumstances. In all examples, unless otherwise stated, Gaussian likelihood functions and uniform prior distributions for the unknowns over given ranges were considered.

2   Results

2.1   Inference of internal Alfvén speed and magnetic field strength

We first applied the Bayesian scheme to the inference of the internal Alfvén speed of coronal loops, considering a particular event described in [5]. Assuming that coronal loops can be modelled as one-dimensional density enhancements in cylindrical geometry and under the thin tube approximation (model M_1), theory relates the observable phase speed, v_{ph}, to the internal Alfvén speed, v_{Ai}, and the density contrast, $\zeta = \rho_{\mathrm{i}}/\rho_{\mathrm{e}}$, in the following manner

$$v_{\mathrm{ph}} \sim v_{\mathrm{Ai}} \left(\frac{2\zeta}{1+\zeta} \right)^{1/2} . \tag{1}$$

Bayes theorem applied to this particular problem tells us that the posterior for the two unknowns, $\theta = \{v_{\mathrm{Ai}}, \zeta\}$ conditional on the measured phase speed, $D = v_{\mathrm{ph}}$, and the assumed model, M_1, is a combination of the likelihood of the data as a function of the unknowns and the prior distributions

$$p(\{v_{\mathrm{Ai}}, \zeta\}|v_{\mathrm{ph}}, M_1) = \frac{p(v_{\mathrm{ph}}|\{v_{\mathrm{Ai}}, \zeta\}, M_1)p(\{v_{\mathrm{Ai}}, \zeta\}|M_1)}{Z_1}, \tag{2}$$

with Z_1 the evidence, a normalisation constant independent of the parameter vector that plays no role in the inference. Considering a Gaussian likelihood function and uniform prior distributions for the unknowns over plausible ranges leads to the marginal posterior shown
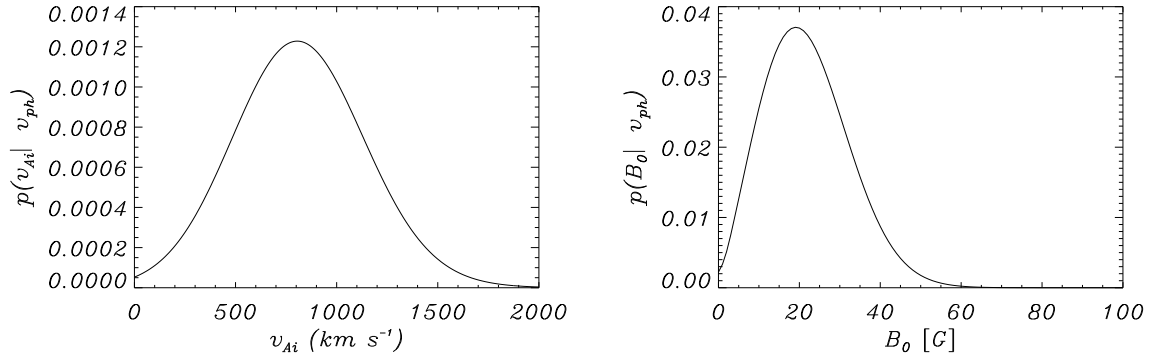
Figure 1: Posterior probability distributions for the internal Alfvén speed (left) and the magnetic field strength (right) for an event with observed phase speed $v_{\mathrm{ph}} = 1030 \pm 410$ km s^{-1} under model M_1, given by Eqs. (1) and (3). The inferred median values for the Alfvén speed and the magnetic field strength are $v_{\mathrm{Ai}} = 813^{+330}_{-317}$ km s^{-1} and $B_0 = 21^{+12}_{-9}$ G respectively, with uncertainties given at the 68% credible interval.

in Fig. 1 (left), which indicates that the internal Alfvén speed can be properly inferred. On the other hand, the density contrast (not shown) cannot be inferred with the information on the phase speed alone.

Equation (1) for the wave phase speed can be expanded to incorporate the magnetic field strength to the inversion. The forward problem for model M_1 can now be formulated as

$$v_{\mathrm{ph}}(\zeta, \rho_{\mathrm{i}}, B_0) = \frac{B_0}{\sqrt{\mu \rho_{\mathrm{i}}}} \left(\frac{2\zeta}{1+\zeta} \right)^{1/2} . \tag{3}$$

In this case, Bayes theorem relates the posterior for three unknowns, $\theta = \{\rho_{\mathrm{i}}, \zeta, B_0\}$ - internal density, density contrast, and magnetic field strength - with the likelihood and prior as

$$p(\{\rho_{\mathrm{i}}, \zeta, B_0\}|v_{\mathrm{ph}}, M_1) = \frac{p(v_{\mathrm{ph}}|\{\rho_{\mathrm{i}}, \zeta, B_0\}, M_1) p(\{\rho_{\mathrm{i}}, \zeta, B_0\}|M_1)}{Z_1} . \tag{4}$$

Figure 1 (right) shows the marginal posterior for the magnetic field strength, which shows a constrained distribution and can therefore be properly inferred. The remaining two parameters, density contrast and internal density cannot be properly inferred and, hence, their posteriors are not shown.

2.2   Information on plasma density

Spectroscopy enables us to obtain some properties of the emitting coronal plasma, such as the density. When additional knowledge like this becomes available, the Bayesian framework offers a self-consistent way to incorporate this additional information to update the posteriors,
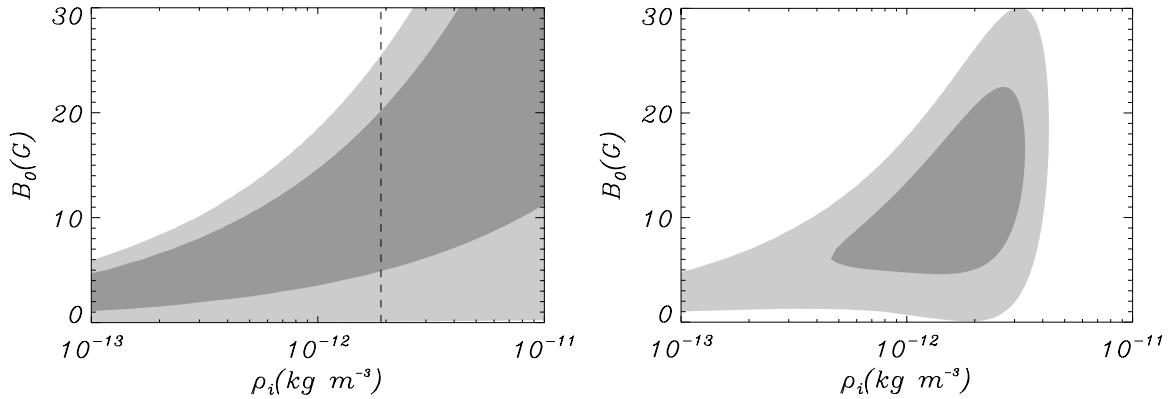
Figure 2:   Comparison between the joint two-dimensional posterior distributions for the internal density of the waveguide and the magnetic field strength obtained for the inference with $v_{\rm ph} = 1030 \pm 410$ km s^{-1}, under model M_1, for the cases of uniform priors (left) and a Gaussian prior for the internal density with $\mu_{\rho_{\rm i}} = 1.9 \times 10^{-12}$ kg m^{-3} and $\sigma_{\rho_{\rm i}} = 0.5\mu_{\rho_{\rm i}}$ (right). The inference with the more informative prior on density leads to $B_0 = 13^{+7}_{-6}$ G and $\rho_{\rm i} = \left(2.2^{+0.9}_{-0.9}\right) \times 10^{-12}$ kg m^{-3}. In both panels, the outer boundaries of the light grey and dark grey shaded regions indicate the 95% and 68% credible regions.

i.e., our state of belief. The proper way to proceed is to consider a more informative prior and to recalculate the posterior.

As an example, assume we have an estimate for the loop density in the previously analysed event, with its corresponding uncertainty. We can use this information to construct a Gaussian prior for the density of the form

$$p(\rho_{\rm i}) = \frac{1}{\sqrt{2\pi\sigma_{\rho_{\rm i}}^2}} \exp\left[-\frac{(\rho_{\rm i} - \mu_{\rho_{\rm i}})^2}{2\sigma_{\rho_{\rm i}}^2}\right], \tag{5}$$

centred on the spectroscopic estimate, $\mu_{\rho_{\rm i}}$, and taking into account its uncertainty, $\sigma_{\rho_{\rm i}}$. The two panels in Fig. 2 show a comparison between the joint posteriors for internal density and magnetic field strength obtained by employing uniform priors (left) and a Gaussian prior on internal density (right), as defined in Eq. (5). As can be seen, the addition of information enables us to further constrain our estimates for both unknowns, waveguide density and magnetic field strength.

2.3   Information on wave damping

Time damping is a commonly observed property in transverse loop oscillations, with characteristic damping times of a few oscillatory periods. The possible influence of this observable on our estimates of the magnetic field strength is unknown. For this reason, we performed the inference including the simplest available model for damping by resonant absorption, a plausible mechanism that seems to explain the observed damping time scales [3]. Resonant damping
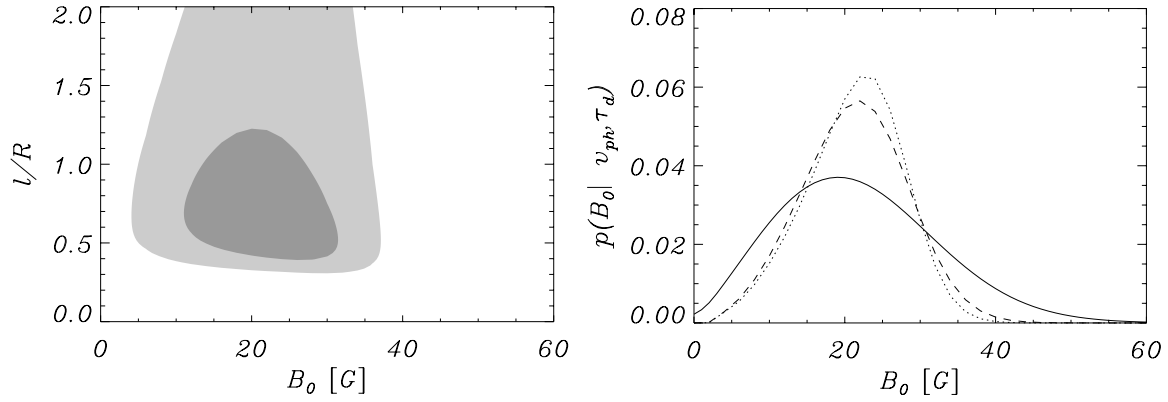
Figure 3:   Left: joint two-dimensional posterior distribution for the magnetic field strength and the transverse density inhomogeneity length-scale obtained for the inference with $v_{\mathrm{ph}} = 1030 \pm 410$ km s^{-1} and $\tau_{\mathrm{d}} = 500 \pm 50$ s, under model M_2 given by Eqs. (6). The outer boundaries of the light grey and dark grey shaded regions indicate the 95% and 68% credible regions. The inferred median values are $B_0 = 21^{+6}_{-7}$ G and $l/R = 1.2^{+0.5}_{-0.4}$, with uncertainties given at the 68% credible interval. Right: a comparison between posteriors for the magnetic field strength for three damping regimes: no damping (solid); $\tau_{\mathrm{d}} = 800 \pm 50$ s (dashed); $\tau_{\mathrm{d}} = 500 \pm 50$ s (dotted).

under the thin tube and thin boundary approximations (model M_2) predicts a relationship between the observable phase speed and damping time and four unknown parameters - internal density, density contrast, magnetic field strength, and transverse inhomogeneity length scale (l/R) - such that

$$v_{\mathrm{ph}}(\rho_{\mathrm{i}}, \zeta, B_0) = \frac{B_0}{\sqrt{\mu\rho_{\mathrm{i}}}} \left(\frac{2\zeta}{1+\zeta} \right)^{1/2} \;\; ; \;\; \tau_{\mathrm{d}}(\rho_{\mathrm{i}}, \zeta, B_0, l/R) = \frac{2}{\pi} \left(\frac{\zeta+1}{\zeta-1} \right) \left(\frac{1}{l/R} \right) \left(\frac{2L}{v_{\mathrm{ph}}} \right), \quad (6)$$

with L the length of the loop.

We first repeated the inference presented in Sect. 2.1, by including some reasonable value for the damping time and using the forward model (6). Bayes theorem now includes additional parameters and observables and can be written as

$$p(\{\rho_{\mathrm{i}}, \zeta, B_0, l/R\}|\{v_{\mathrm{ph}}, \tau_{\mathrm{d}}\}, M_2) = \frac{p(\{v_{\mathrm{ph}}, \tau_{\mathrm{d}}\}|\{\rho_{\mathrm{i}}, \zeta, B_0, l/R\}, M_2)p(\{\rho_{\mathrm{i}}, \zeta, B_0\}|M_2)}{Z_2}. \quad (7)$$

An example inversion result is shown in Fig. 3 (left), which displays the joint probability distribution for magnetic field strength and transverse density inhomogeneity length scale. Both parameters can be well constrained.

The posterior for the magnetic field strength shows a more constrained shape, in comparison to the inversion without the use of the damping time (Sect. 2.1). The median of the

probability density is the same as in the case without damping, but the dispersion is smaller. This is more clearly seen in Fig. 3 (right), were posteriors for the magnetic field strength for different damping regimes are displayed. These results point to the importance of considering the information on the damping time scale of coronal loop oscillations, when inferring the magnetic field strength, because the seismic variables are coupled through the forward model given by Eqs. (6).

3   Conclusions

The magnetic field strength in transversely oscillating coronal waveguides can be inferred, even if the densities inside and outside and their ratio are largely unknown. When spectroscopic information on plasma density is available, the method enables to incorporate this knowledge in a self-consistent manner, further constraining the inference. The observed oscillation damping is relevant and should be incorporated to the inversion procedure. First, it enables to obtain information on the transverse inhomogeneity length scale of the density at the boundary of the waveguide, a parameter directly related to wave heating mechanisms. Second, its consideration produces posteriors for the magnetic field strength that differ appreciably from those obtained with the information on the phase speed alone. The methods here presented can in principle be applied to another magnetic and plasma structures in the solar atmosphere, such as prominence fine structures or chromospheric spicules.

Acknowledgments

References

[1] Arregui, I., Andries, J., Van Doorsselaere, T., Goossens, M., & Poedts, S. 2007, A&A, 463, 333

[2] Aschwanden, M. J., Fletcher, L., Schrijver, C. J., & Alexander, D. 1999, ApJ, 520, 880

[3] Goossens, M., Andries, J., & Aschwanden, M. J. 2002, A&A, 394, L39

[4] Nakariakov, V. M. & Ofman, L. 2001, A&A, 372, L53

[5] Nakariakov, V. M., Ofman, L., DeLuca, E. E., Roberts, B., & Davila, J. M. 1999, Science, 285, 862

[6] Roberts, B., Edwin, P. M., & Benz, A. O. 1984, ApJ, 279, 857

[7] Rosenberg, H. 1970, A&A, 9, 159

[8] Uchida, Y. 1970, PASJ, 22, 341